ISSN 1063-7834, Physics of the Solid State, 2016, Vol. 58, No. 10, pp. 2055–2061. © Pleiades Publishing, Ltd., 2016.
Original Russian Text © P.A. Rodnyi, K.A. Chernenko, A. Zolotarjovs, L. Grigorjeva, E.I. Gorokhova, I.D. Venevtsev, 2016, published in Fizika Tverdogo Tela, 2016, Vol. 58, No. 10, pp. 1982–1988.

IMPURITY CENTERS

Effect of Point Defects on Luminescence Characteristics of ZnO Ceramics

P. A. Rodnyi[a], K. A. Chernenko[a]*, A. Zolotarjovs[b], L. Grigorjeva[b], E. I. Gorokhova[c], and I. D. Venevtsev[a]

[a] *Peter the Great Saint-Petersburg Polytechnic University, ul. Polytekhnicheskaya 29, St. Petersburg, 195251 Russia*
[b] *Institute of Solid State Physics, University of Latvia, 8 Kengarga st., Riga, LV-1063 Latvia*
[c] *Research and Technological Institute of Optical Materials Studies, Vavilov Optical Institute, St. Petersburg, 193171 Russia*
** e-mail: nuclearphys@yandex.ru*

Received December 14, 2015; in final form, March 17, 2016

Abstract—Photo- and thermally stimulated luminescence of ZnO ceramics are produced by uniaxial hot pressing. The luminescence spectra of ceramics contain a wide band with a maximum at 500 nm, for which oxygen vacancies V_O are responsible, and a narrow band with a maximum at 385 nm, which is of exciton nature. It follows from luminescence excitation spectra that the exciton energy is transferred to luminescence centers in ZnO. An analysis of the thermally stimulated luminescence curves allowed detection of a set of discrete levels of point defects with activation energies of 25, 45, 510, 590 meV, and defects with continuous energy distributions in the range of 50–100 meV. The parameters of some of the detected defects are characteristic of a lithium impurity and hydrogen centers. The photoluminescence kinetics are studied in a wide temperature range.

DOI: 10.1134/S1063783416100309

1. INTRODUCTION

Zinc oxide (ZnO) as a wide band-gap semiconductor (band gap $E_g = 3.37$ eV) with unique optical properties causes great interest for researchers [1, 2]. Two emission bands are observed in various zinc oxide forms: single crystals, thin films, nanocrystals, and ceramics: one is a short-wavelength band near the crystal absorption edge, i.e., band-edge luminescence; and the second is a broad long-wavelength band whose maximum is usually in the green spectral region. Band-edge luminescence with a maximum at 3.35 eV and a decay time of ~0.7 ns is of exciton nature [1]. The long-wavelength band results from electron recombination at luminescence centers, i.e., zinc vacancies V_{Zn} [3], oxygen vacancies V_O [4], and other defects (so-called intraband luminescence) [1, 2]. Later on, it became clear that the broad green luminescence (GL) band can consist of two bands: in samples with excess oxygen, the GL maximum is at E_m = 2.30 eV (half-width at half maximum $\Delta E_{1/2}$ = 450 meV); in samples with excess zinc, $E_m = 2.52$ eV, $\Delta E_{1/2} = 340$ meV [5, 6]. In the case of oxygen excess, recombination occurs between the conduction band electron and an acceptor, i.e., the zinc vacancy V_{Zn}; in the case of zinc excess, recombination occurs between the valence band hole and V_O donor [5]. It is natural that interstitial oxygen centers O_i and interstitial zinc centers Zn_i are formed in O- and Zn-excess samples [6], respectively. In most cases, Zn-excess samples are obtained, which contain interstitial zinc being the shallow donor; therefore, ZnO crystals have *n*-conductivity type [1, 6]. Shallow donors in ZnO can also be hydrogen ions H^+ [1].

Deep and fine point defects have a significant effect on electrical and luminescence characteristics of zinc oxide. Properties of defects and impurities in ZnO were studied by thermally stimulated luminescence (TSL) [4], electron paramagnetic resonance (EPR) [7, 8], and photocapacitance measurements [9]. There are also theoretical studies generalized in [10]. Special difficulties are caused by the study of shallow defects (electron traps with depths of tens of millielectrovolts); in this case, a special electron spectroscopy [9] or low-temperature TSL [11] methods are used. In ZnO single crystals, two types of shallow donors with depths of 30 and 60 meV were detected [12]; then, it was shown that it is the same donor in ground (D^0) and excited (D^*) states [3]. It is also assumed that the interstitial zinc ion Zn_i is this donor [13, 14]. It was also shown that, depending on the ZnO sample growth method, it can contain electron traps with a depth of 30–80 meV [14].

A comprehensive review of the published data on zinc oxide properties is given in [1, 15]. Main studies

of luminescence features and point defects were performed on single crystals. The studies of ceramics are mostly devoted to their electrical properties (see, e.g., the review [16]), since zinc oxide is a widely accepted material for producing varistors. Works directed to the study of luminescence properties of ceramics are scarce and contain information on synthesis parameters [17–20], emission spectra [17–20], and luminescence decay kinetics [21, 22].

In the present work, point defects in ZnO ceramics were studied by the TSL method. The TSL curves were measured with a wavelength resolution in a wide temperature range. Luminescence characteristics, i.e., the emission and excitation spectra and decay kinetics, of ceramics were also studied.

2. SAMPLE PREPARATION AND EXPERIMENTAL TECHNIQUE

Ceramics were produced by uniaxial hot pressing in a high-temperature vacuum furnace [23]. As a source material, domestic ZnO powder (ultra-pure grade) was used. Characteristics of initial powders (dispersion and morphological composition) of obtained ceramics are described in [23]. The average grain size in ceramics was 5–30 μm. The samples shaped as disks 24 mm in diameter after mechanical treatment were from 0.4 to 1.5 mm thick. The total transmission of ZnO samples 0.4 mm thick in the visible spectral region was 50–65%, i.e., optical ceramics were obtained. The TSL curves were measured using a setup based on a helium closed-cycle cryostat. As a detector, an Andor Shamrock B-303i-B monochromator with an attached Andor IDus CCD camera was used, which allowed TSL signal measurements with wavelength resolution.

The samples were exposed to X-rays (45 kV, 15 mA) for 30 min at a temperature of 10 K, and then were heated with a rate of 0.1 K/s to 300 K. For high-temperature well-resolved peaks, the main parameters of charge traps, i.e., the center activation energy E_a, the kinetics order, and the frequency factor, were determined by the known Chen formula [24]. In the case of incomplete thermal peak resolution, the trap depth was determined by the fractional heating method [25].

The photoluminescence (PL) spectra and PL decay curves were measured by the time-correlated single-photon counting (TCSPC) method. A CryLas type 1Q266-1 pulsed laser with a pulse energy of 0.3 μJ and a pulse duration of 1 ns was used for excitation. Radiation was recorded using a Hamamatsu H8259-2 photodetector and a FAST ComTec P7887 time–code conversion card with a time resolution of 250 ps. The sample was placed in a closed-cycle helium cryostat in the reflection-mode position. A required wavelength was separated using an MDR-3 monochromator, correction for photodetector sensitivity was not performed.

Excitation spectra were measured in a vacuum nitrogen cryostat; a LOT-ORIEL xenon lamp of power 150 W was used as an excitation source; necessary excitation and radiation wavelengths were separated using MDR-3 and ORIEL Corner Stone 1/8 m monochromators, respectively; a Hamamatsu 8259 counting head was a photodetector. Measurements were performed in the reflection mode.

3. EXPERIMENTAL RESULTS

The luminescence spectra of ZnO ceramics are shown in Fig. 1a. The PL band has a maximum at ~500 nm, the bandwidth increases with temperature. The structure of the band indicated in some studies [1, 13] was not observed in the case at hand even at 15 K. Furthermore, it was also impossible to detect the structure in measuring time-resolved spectra. The maximum of the edge (exciton) band shifts from 368 nm at 15 K to 377 nm at 300 K.

The fundamental PL band excitation band is in the energy range smaller than the band gap (Fig. 1b). Its maximum shifts from 382 nm at 80 K to 390 nm at 300 K, and the half-width increases with temperature. It is significant that the PL excitation efficiency is low in the energy (wavelength) range corresponding to interband transitions. We note that no shift of the maximum or change in the emission spectrum half-width were detected with varying the excitation wavelength.

Figure 2a shows the TSL curves of ceramics for various wavelengths. The strongest TSL maximum is recorded at 35 K. In the temperature range from 50 to 150 K, gently sloping luminescence, i.e., a "plateau", is observed. Two maxima were observed in the high-temperature region, 230 and 290 K. In the range of 15–90 K, TSL was also studied by the fractional heating method which allowed the determination of the corresponding activation energies (see the inset in Fig. 2a).

Figure 2b shows the TSL spectra of ZnO ceramics at various temperatures, normalized to the maximum intensity. We can see that the obtained spectra differ significantly from each other, which indicates different luminescence mechanisms in thermal peaks. The broad ($\Delta E_{1/2} = 0.5$ eV) luminescence band with a maximum at 614 nm is characteristic of the low-temperature peak (Fig. 2b, curve *1*). The luminescence band with $\lambda_m \sim 510$ nm corresponds to the temperature range of 50–150 K (Fig. 2b, curve *2*). At a temperature of 170 K, in addition to PL, a band with $\lambda_m = 730$ nm is recorded in the red region (Fig. 2b, curve *3*). For the thermal peak at 230 K (Fig. 2b, curve *4*), PL with $\lambda_m \sim$ 510 nm is characteristic (the spectral peak at 290 K coinciding with it is not shown in Fig. 2b). For comparison, Fig. 2b shows the X-ray luminescence spectrum measured at a temperature of 10 K.

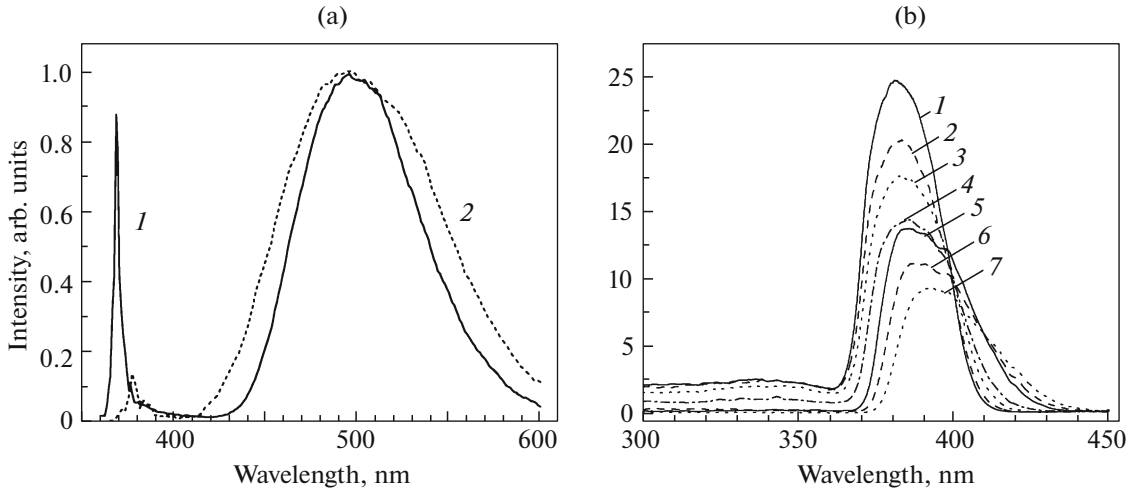

Fig. 1. (a) PL spectra (λ_{exc} = 266 nm) of ZnO ceramics at (*1*) 15 and (*2*) 300 K; (b) 500-nm band luminescence excitation spectra at temperatures of (*1*) 80, (*2*) 100, (*3*) 140, (*4*) 180, (*5*) 260, (*6*) 300, and (*7*) 340 K.

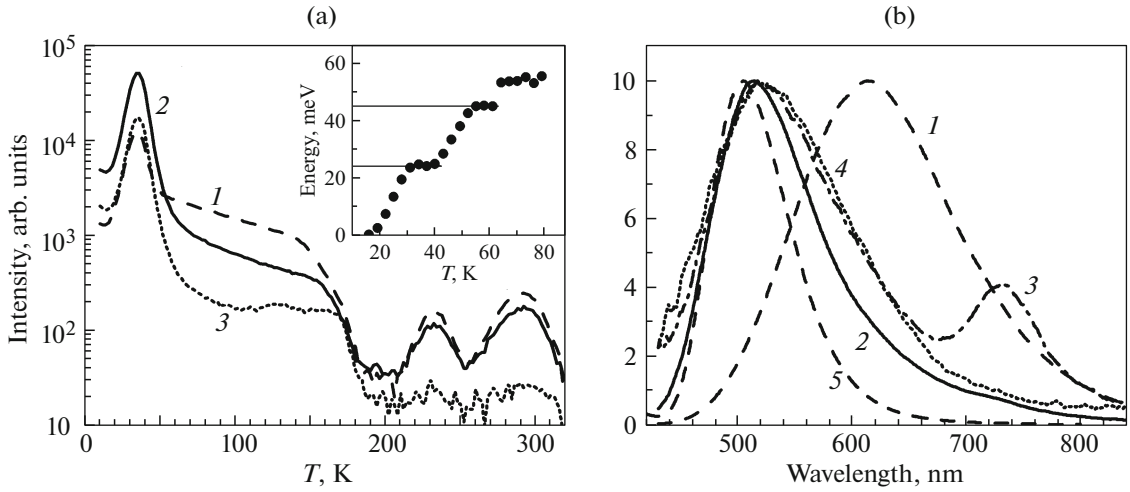

Fig. 2. (a) TSL curves measured at wavelengths of (*1*) 525, (*2*) 620, and (*3*) 730 nm. The inset shows the activation energy determination by the fractional heating method; (b) TSL spectra of ZnO ceramics measured at temperatures of (*1*) 35, (*2*) 80, (*3*) 170, and (*4*) 230 K and (*5*) the X-ray luminescence spectrum measured 10 K.

The results of measurements of PL kinetic curves (λ_{em} = 500nm) are shown in Fig. 3. All decay curves exhibit a complex decay behavior which cannot be described by the exponential law characteristic of intracenter luminescence.

To consider the features of the temperature evolution of the luminescence decay kinetics in more detail, we divided it into three time intervals: 0–20 ns, 20 ns–5 μs, and 5–100 μs. From 0 to 20 ns, the fast luminescence decay component is observed, which can be roughly approximated by exponential decay with a slope constant of ~5 ns. For the time interval of 20 ns–5 μs, the exponential decay with a constant of 680 ns at a temperature of 20 K is characteristic. At $t > 5$ μs, the slow kinetics with nonexponential decay behavior law is observed.

The decay time of the fast luminescence component is almost independent of temperature. The intensity of the exponential luminescence component with constant τ = 680 ns decreases with increasing temperature (see the inset in Fig. 3), whereas the relative intensity of the slow luminescence component increases, which results in a general kinetics inhibition. As the temperature increases above 200 K, the characteristic time of the slow luminescence component (>5 μs) also decreases.

To estimate the luminescence intensity, the kinetic curves obtained under the same conditions were

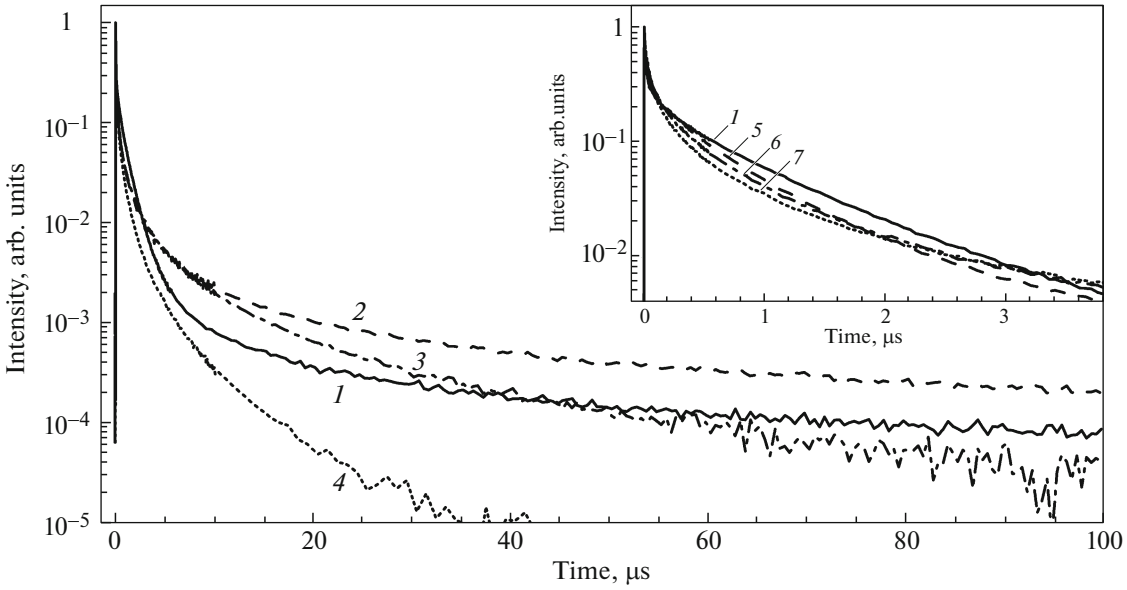

Fig. 3. PL decay kinetics of ZnO ceramics (λ_{exc} = 500 nm) at temperatures of (*1*) 20, (*2*) 150, (*3*) 250, and (*4*) 300 K. The inset shows the initial portion of the PL decay kinetics at temperatures of (*1*) 20, (*5*) 45, (*6*) 75, and (*7*) 100 K. The curve intensity is normalized.

numerically integrated. The integration results are shown in Fig. 4.

4. RESULTS AND DISCUSSION

4.1. Emission and Excitation Spectra

The obtained luminescence maximum position ($\lambda_m \sim 500$ nm, $\Delta E_{1/2} = 400$ meV at 15 K) corresponds to radiation characteristics of samples produced in a reducing atmosphere [5, 6]. It is assumed that oxygen vacancies V_O are dominant luminescence centers in this case.

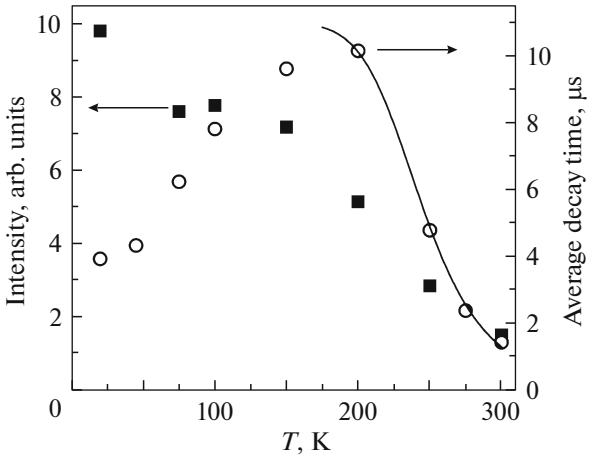

Fig. 4. Temperature dependences of the total luminescence intensity (squares) and the average luminescence time (circles). The curve is the approximation of the average luminescence decay time by the Mott formula.

The band-edge luminescence band position (368 nm at 15 K) and its temperature dependence suggest that donor-bound excitons D^0X are responsible for measured radiation [9]. The shift of the maximum of this band to the short-wavelength spectral region with decreasing temperature (Fig. 1a) is caused by a corresponding band gap widening (E_g = 3.437 eV at 1.6 K and E_g = 3.37 eV at 300 K [1]) and a shift of the ZnO fundamental absorption edge. Thus, luminescence characteristics of studied optical ceramics appeared close to those for ZnO single crystals [9, 13].

Luminescence with a maximum at 500 nm is efficiently excited in the region of energies lower than the band gap; in this case, the excitation band maximum shifts to the short-wavelength region with decreasing temperature, similarly to the band-edge luminescence maximum (Fig. 1a). To explain this behavior of excitation spectra, two models were previously proposed. In the first model proposed based on an analysis of the data on optical detection of the magnetic resonance [8], the energy transfer occurs via intermediate free and donor-bound exciton states. In the second model [14], valence band electrons after optical excitation are transferred to the levels caused by shallow donors; then, being thermally released, appear at luminescence centers. It should be noted that the ratio of the intensity at the PL excitation band maximum to the excitation intensity in the interband transition region in the ceramics under study is significantly higher than in [14, 26, 27]. This points to a higher concentration of donors and defect states in ceramics.

4.2. Thermally Stimulated Luminescence

The trap parameters determined by analyzing the TSL curves and their comparison in the published data available for crystals are listed in the table.

When analyzing the peak with a maximum at 35 K, the activation energy of 25 meV and the frequency factor of 1500 s^{-1} were determined by the Chen method. The TSL in this temperature region was also studied using the fractional heating method (see the inset in Fig. 2a), which allowed, along with the primary defect with an activation energy of 25 meV, detection of an additional defect with an activation energy of 45 meV.

The strong low-temperature (35 K) TSL peak of ZnO ceramics (Fig. 2a) was also recorded in single crystals [4, 28, 29]. The emission band peak maximum (λ_m = 614 nm) is in the yellow spectral region (Fig. 2b, curve *1*), which indicates the difference of the low-temperature TSL mechanism from PL (green spectral region). In this case, yellow luminescence with a maximum at 2.2 eV was recorded in both the crystals containing a lithium impurity [9, 26, 28, 29] and impurity-free ZnO samples [31]. It is believed that (along with lithium acceptor in doped samples) the luminescence center for the band of 2.2 eV can be interstitial oxygen O_i whose ground level is in the crystal band gap slightly higher than the oxygen vacancy level [32].

The trap parameters we obtained for the peak with a maximum at 35 K are in agreement with the results of [28], among other factors, confirm the extraordinarily low frequency factor uncharacteristic of phonon frequencies. The low frequency factor can be explained by tunneling processes involved in TSL. For example, simultaneous measurements of thermally stimulated conductivity (TSC) and TSL [29] revealed the absence of the corresponding TSC peak at 35 K, i.e., electron tunneling from electron trap level to luminescence centers occurs, rather than thermal ionization of shallow donors. The existence of such processes was convincingly shown for lutetium silicate crystals activated by cerium [33]. In this case, the activation energy corresponds to the energy difference between the ground and excited donor levels, rather than to the gap between the bottom of the conduction band and the donor energy level.

The TSL peak curve shape at 35 K corresponds to the second-order kinetics, which is probably caused by the luminescence peak with an activation energy of 45 meV, overlapped with the TSL peak. Shallow donors were detected in ZnO by various methods [4, 9, 11]; however, there is no consensus about the nature of these centers. In high-quality ZnO single crystals, donor levels with depths of 23 [9], 36, 47, and 55 meV [11] are attributed to various hydrogen centers.

The long gentle slope of TSL curves in the temperature range from 50 to 150 K was recorded in ZnO crystals with a lithium impurity. Such a curve shape is not consistent with classical models developed for electron traps with a discrete energy level. The possible explanation of such a curve shape is the existence of the continuous distribution of traps over energies or frequency factors due to distorted parameters of traps of one type by the Coulomb field caused by the interaction with other defects [28, 34]. A similar plateau was also observed in some ZnO crystals nominally containing no lithium impurities [4]. Nevertheless, lithium is a typical impurity in the hydrothermal method for growing ZnO crystals; therefore, such a characteristic TSL curve can indicate the presence of a residual lithium impurity not controlled experimentally. Thus, the existence of donor levels in the range from 50 to 100 meV should be assumed for ZnO ceramics. In this case, the TSL spectrum (curve *2*, Fig. 3) corresponds to emission of V_O centers.

Electron traps parameters in ZnO ceramics: T_m is temperature at the thermal peak maximum, E_a is the activation energy, b is the kinetics order, s is the frequency factor, and λ_m is the wavelength at the TSL spectrum maximum*

T_m, K	E_a, meV	b	s, s^{-1}	λ_m, nm
35	25	2.0	1.5×10^3	614
	23 [9]; 30 [29]	2.0 [28]	10^2 [28]	600 [4]
55	45	1		614
50–150	80 [28]		10^2 [28]	510
230	590	1.6	10^{11}	520
	600 [28]		10^{12} [28]	
290	510	1.0	10^7	520
	500 [30]			

* The bottom lines are the literature data.

The TSL spectrum in the region of 170 K (curve *3*, Fig. 3) contains a band with λ_m = 730 nm in the red spectral region in addition to PL ($\lambda_m \approx$ 520 nm). Such luminescence was also recorded in ZnO single crystals [4]; it is attributed to transitions between various charge states of oxygen vacancies. The high-temperature peaks at 230 and 290 K were also detected in crystals [28, 30]; they are associated with electron release from deep (500–600 meV) traps (see the table).

4.3. Luminescence Decay Kinetics

Since the measured luminescence decay curves were nonexponential, the luminescence decay kinetics was quantitatively described using the average luminescence time

$$\bar{t} = \frac{\int tI(t)dt}{\int I(t)dt},$$

where $I(t)$ is the time dependence of the luminescence intensity. To determine the average luminescence time, experimental curves were numerically integrated

in the range of 0–100 μs; the results are shown in Fig. 4. As the temperature increases, the average luminescence time initially increases, and then, beginning with 200 K, decreases.

The complex shape of luminescence decay curves is observed in various ZnO forms [22, 26, 35–38]; the characteristic decay times vary depending on sample synthesis conditions, exciting radiation type, and excitation pulse duration. For comparison, the average luminescence time of ZnO powder, calculated by the data of [26] under the closest excitation conditions are 31 μs ($T = 250$ K, $E_{exc} = 3.54$ eV); whereas the result we obtained is 4.8 μs ($T = 250$ K, $E_{exc} = 4.66$ eV).

Despite the significant differences in the characteristic luminescence time, the kinetic behavior with temperature is similar in various ZnO forms [26, 39, 40]: an anomalous increase in the luminescence decay time with temperature is observed. To explain this phenomenon, a model was proposed in [26] in which electrons appearing in the conduction band due to thermal ionization of shallow donors are sources of the slow luminescence component.

The decrease in the luminescence time as the temperature increases above 200 K at a simultaneous decrease in the intensity is characteristic of thermal quenching of ZnO luminescence. The activation energy obtained by approximating this decay by the Mott formula is 230 meV. Such an energy characteristic of the PL center was also measured in [26, 27].

5. CONCLUSIONS

The luminescence band with a maximum at 500 nm, characteristic of ZnO produced in a reducing atmosphere, dominates in the emission spectrum of studied ceramics. The band-edge luminescence band has a relatively low intensity due to overlapping of its emission band and the PL excitation band. In studied ceramics, the excitation band half-width and the ratio of the intensity at the PL excitation band maximum to the excitation intensity in the region of interband transitions is significantly larger than in single crystals, which indicates a larger number of defect states probably accumulated at the grain boundaries in ceramics.

Among the set of defects in ZnO ceramics, detected by the TSL method, the residual lithium impurity plays the greatest role. In this case, two different luminescence mechanisms are associated with lithium: one involving tunneling processes (luminescence with a maximum at 614 nm) and carrier release to the conduction band (luminescence with a maximum at 510 nm). The high TSL intensity has an adverse effect on luminescence properties; therefore, the lithium impurity should be carefully controlled in further studies.

The green luminescence decay kinetics in which the average luminescence time increase with temperature is presumably associated with carrier release from traps. The temperature range where the decay kinetics time increases contains a TSL "plateau" associated with the continuous energy distribution of defects in the band gap, which probably does lead to the complex shape of the luminescence decay curves.

REFERENCES

1. Ü. Özgür, Ya. I. Alivov, C. Liu, A. Teke, M. A. Reshchikov, S. Doğan, V. Avrutin, S.-J. Cho, and H. Morkoçd, J. Appl. Phys. **98**, 041301 (2005).
2. D. G. Thomas, J. Phys. Chem. Solids **15**, 86 (1960).
3. H. Chen, S. Gu, K. Tang, S. Zhu, Zh. Zhu, J. Ye, R. Zhang, and Y. Zheng, J. Lumin. **131**, 1189 (2011).
4. Y. Wang, B. Yang, N. Can, and P. D. Townsend, J. Appl. Phys. **109**, 053508 (2011).
5. C. Ton-That, L.Weston, and M. R. Phillips, Phys. Rev. B: Condens. Matter **86**, 115205 (2012).
6. T. Moe Berseth, B. G. Svenson, A. Yu. Kuznetsov, P. Klason, Q. X. Zhao, and M. Willander, Appl. Phys. Lett. **89**, 262112 (2006).
7. D. M. Hoffmann, A. Hofstaetter, F. Leiter, H. Zhou, F. Henecker, B. K. Meyer, S. B. Orlinskii, J. Schmidt, and P. G. Baranov, Phys. Rev. Lett. **88**, 045504 (2002).
8. F. Leiter, H. Alves, D. Pfisterer, N. G. Romanov, D. M. Hofmann, and B. K. Meyer, Physica B (Amsterdam) **201**, 340 (2003).
9. C. Ton-That, L. L. C. Lem, M. R. Phillips, F. Reisdorffer, J. Mevellec, T.-P. Nguyen, C. Nenstiel, and A. Hoffmann, New J. Phys. **16**, 083040 (2014).
10. F. Oba, M. Choi, A. Togo, and I. Tanaka, Sci. Technol. Adv. Mater. **12**, 034302 (2011).
11. Ji Jianfeng, L. A. Boatner, and F. A. Selim, Appl. Phys. Lett. **105**, 041102 (2014).
13. D. C. Reynolds, D. C. Look, and B. Jogai, J. Appl. Phys. **89**, 6189 (2001).
14. K. Kodama and T. Uchino, J. Appl. Phys. **111**, 093525 (2012).
15. C. Klingshirn, J. Fallert, H. Zhou, J. Sartor, C. Thiele, F. Maier-Flaig, D. Schneider, and H. Kalt, Phys. Status Solidi B **247**, 1424 (2010).
16. K. Tapan and J. Gupta, Am. Ceram. Soc. **73** 1817 (1990).
17. V. I. Kushnirenko, I. V. Markevich, and A. V. Rusavsky, Radiat. Meas. **45**, 468 (2010).
18. R. C. Hoffmann and J. J. Schneider, J. Am. Ceram. Soc. **94**, 1878 (2011).
19. M. Hong, D. Fredrick, D. M. Devito, J. Y. Howe, Xia Yang, N. C. Giles, J. S. Neal, and Zu. A. Munir, Int. J. Appl. Ceram. Technol. **8**, 725 (2011).
20. I. V. Markevich and V. I. Kushnirenko, Solid State Commun. **149**, 866 (2009).
21. Wen Xiao-ming, N. Ohno, and Zh. Zhong-ming, Chin. Phys. **10**, 874 (2001).
22. L. Grigorjeva, D. Millers, J. Grabis, J. Fidelus, W. Lojkowski, T. Chudoba, and K. Bienkowski, Radiat. Meas. **45**, 441 (2010).
23. E. I. Gorokhova, P. A. Rodnyi, K. A. Chernenko, G. V. Anan'eva, S. B. Eron'ko, E. A. Oreshchenko,

I. V. Khodyuk, E. P. Lokshin, G. B. Kunshina, O. G. Gromov, and K. P. Lott, Opt. Zh. **78**, 85 (2011).

24. R. Chen and V. Pagonis, *Thermally and Optically Stimulated Luminescence: A Simulation Approach* (Wiley, New York, 2011).
25. I. Kudryavtseva, A. Lushchik, A. I. Nepomnyashchikh, F. Savikhin, E. Vasil'chenko, and Yu. Lisovskaya, Phys. Solid State **50** (9), 1667 (2008).
26. K. Kodama and T. Uchino, J. Phys. Chem. C **118**, 23977 (2014).
27. J. V. Foreman, J. G. Simmons, W. E. Baughman, J. Liu, and H. O. Everitt, J. Appl. Phys. **113**, 133513 (2013).
28. D. Zwingel, J. Lumin. **5**, 385 (1972).
29. G. Baur, E. V. Freydorf, and W. H. Koschel, Phys. Status Solidi A **21**, 247 (1974).
30. Y. P. Tu, Q. Wang, J. He, X. Li, and L. J. Ding, Sci. China Tech. Sci. **56**, 677 (2013).
31. A. B. Djurisic, Y. H. Leung, K. H. Tam, L. Ding, W. K. Ge, H. Y. Chen, and S. Gwo, Appl. Phys. Lett. **88**, 103107 (2006).
32. M. Willander, O. Nur, J. R. Sadaf, M. I. Qadir, S. Zaman, A. Zainelabdin, N. Bano, and I. Hussain, Materials **3**, 2643 (2010).
33. A. Vedda, M. Nikl, M. Fasoli, E. Mihokova, J. Pejchal, M. Dusek, G. Ren, C. R. Stanek, K. J. McClellan, and D. D. Byler, Phys. Rev. B: Condens. Matter **78**, 195123 (2008).
34. E. M. Zobov, M. E. Zobov, and S. P. Kramynin, J. Appl. Spectrosc. **77** (6), 841 (2011).
35. W. Xiao-ming, N. Ohno, and Zh. Zhong-ming, Chin. Phys. **10**, 874 (2001).
36. L. Grigorjeva, D. Millers, A. Kalinko, V. Pankratov, and K. Smits, J. Eur. Ceram. Soc. **29**, 255 (2009).
37. H. Haiping, Ye Zhizhen, L. Shisheng, Zh. Binghui, H. Jingyun, and T. Haiping, J. Phys. Chem. C **112**, 14262 (2008).
38. M. Nikl, G. P. Pazzi, P. Fabeni, E. Mihokova, J. Pejchal, D. Ehrentraut, A. Yoshikawa, and R. T. Williams, J. Lumin. **129**, 1564 (2009).
39. A. van Dijken, E. A. Meulenkamp, D. Vanmaekelbergh, and A. Meijerink, J. Phys. Chem. B **104**, 1715 (2000).
40. H. He, Z. Ye, S. Lin, B. Zhao, J. Huang, and H. Tang, J. Phys. Chem. C **112**, 14262 (2008).

Translated by A. Kazantsev